institut de physique nucleaire

Submitted to Physical Review C.

DEEXCITATION OF NUCLEI FORMED NEAR THE INSTABILITY TEMPERATURE*

M.F. Rivet, B. Borderie, H. Gauvin, D. Gardès, C. Cabot
Institut de Physique Nucléaire, Orsay, FRANCE

F. Hanappe
FNRS and Université Libre de Bruxelles, BELGIUM

and J. Peter
GANIL, Caen, FRANCE

ABSTRACT

Fusion-like reactions induced on medium mass targets by 27 MeV per nucleon argon projectiles were studied. The properties of evaporation residues and binary fission fragments, both cold remnants of fusion nuclei, show that highly excited nuclei were produced, near the temperature of instability of nuclear matter. Fission-evaporation competition in the deexcitation of these nuclei is reflected in the ratio of fission and residue cross sections, which provides a way of studying the role of prefission evaporation and fission barriers in the deexcitation process.

* Experiment performed at Ganil - Caen (France)

I INTRODUCTION

The fusion process between two heavy ions has been extensively studied at low incident energies ; it occurs for central collisions and is characterized by a complete transfer of linear and angular momentum, and the total available energy is transformed into excitation energy. The deexcitation of fusion nuclei is rather well known and proceeds through particle evaporation, or fission, or both, with relative probabilities well described by a statistical model[1-2]. As the incident energy increases, direct high energy light particles are observed, most likely emitted at an early stage of the reaction. They take away part of the incident linear and angular momentum, and part of the available energy. This phenomenon is known as incomplete fusion, or fusion-like process and, following various models, direct particles are said to originate from hot spots[3-4], or Fermi-jets[5-7], or preequilibrium processes[8-11]. The onset of direct particle emission occurs for relative velocities at contact around c/10 (typically 7-8 MeV per nucleon for Ar projectiles on medium targets). The increase of direct particle multiplicity with incident energy is correlated with a decrease of the average percentage of linear momentum transferred (LMT) to fusion-like nuclei. This effect is clearly seen on the systematic pattern of LMT to fusion-like nuclei with masses larger than 100, produced by an extensive set of projectiles ranging from ^{4}He to ^{40}Ar[12-13]. The decrease of LMT is roughly linear up to incident energies around 30 MeV per nucleon. Above this energy a dependence of LMT on projectile mass seems to appear[14-16]. This raises the question of the role of excitation energy on fusion processes, as for a given relative velocity the excitation energy will increase with

projectile mass. A comparison[17] of fusion-like reactions induced by Ar projectiles on various targets from Al to U[13-15,18-21] shows a gradual decline of fusion processes when the excitation energy brought into the fusion nuclei reaches a maximum limit. Expressed in MeV per nucleon, this limit is higher for light systems than for heavy ones, in good agreement with critical excitation energies predicted by theoretical studies of the static properties of highly excited nuclei[22-24] or energy thresholds for multifragmentation[25].

The limiting excitation energies are very high, corresponding in all cases to temperatures larger than 5 MeV. Therefore incomplete fusion reactions induced by projectiles such as Ar between 20 and 30 MeV per nucleon provide a unique way to study the deexcitation of very hot nuclei. Important questions can be addressed, concerning the fission-evaporation competition or cluster evaporation (Li → Ne), for example. Indeed it has been known for several years that classical statistical models already fail to explain prefission particle evaporation observed for Ar induced reactions at 8 MeV per nucleon[26]. What happens at much higher temperatures remains an open question.

In this paper the reactions induced by 27 MeV per nucleon argon projectiles on silver and holmium targets are reported. Such medium mass systems are the best to study fission-evaporation competition for fusion-like nuclei, which happened to be produced at excitation energies very near the critical value. Partial results on the Ar + Ag system have already been published[27], concerning essentially heavy fusion residues. These results are now completed by the fusion-fission data. After the experimental technique (sect. II), the heavy residue and fission results (sect. III) are presented, followed by a discussion of the characteristics of fusion-like processes (sect. IV).

Then fission-evaporation competition is quantitatively analyzed in light of recent calculations. In the last section the possible signature of heavy cluster evaporation in the residue angular distributions is discussed , with the help of a Monte-Carlo simulation.

II EXPERIMENT

The 1090 MeV ^{40}Ar beam was delivered by the Ganil facility. The beam direction was precisely defined by monitoring the elastic scattering on both sides of the beam. Thin targets of natural silver and holmium were used, in order to minimize the experimental velocity threshold. The silver target (270 $\mu g/cm^2$ areal density) was self-supporting whereas the holmium target (210 $\mu g/cm^2$) was deposited onto a 256 $\mu g/cm^2$ aluminum backing. A thicker silver target (930 $\mu g/cm^2$) was used to study the fission correlations, to improve the statistics.

Reaction products were detected by means of a time-of-flight telescope subtending a solid angle of 7×10^{-5} sr. The flight path was equal to 1.25 m, and an angular range from 6 to 50° was explored. The stop detector was a 150 µm low-resistivity surface barrier detector, whereas the start detector consisted of a thin carbon foil associated with channel plates. Magnesium oxide was evaporated on the carbon foil to increase detection efficiency of products for which the stopping power of carbon is small.

Fission correlations were studied by detecting the coincident partner in a large area (20 x 20 cm^2) parallel plate avalanche counter (PPAC), located on the other side of the beam. In addition to the time-of-flight difference between the coincident fragments, the PPAC provided the in and out-of-plane angles of the second fragment through

two localization signals. The TOF telescope was then set at 20° (Ag target) and 25° (Ho target) ; these angles were carefully chosen to prevent any kinematical bias when detecting fission following the largest linear momentum transfers. Two positions of the PPAC were necessary in each case to cover the whole fission correlation.

The beam intensity, typically 100 electricalnA when performing singles measurements, was reduced to 15 nA during the fission coincidence measurements, to avoid excessive counting rates on the PPAC. Moreover the electron noise, visible on all signals from this detector, was satisfactorily decreased by applying a high voltage on the target ladder (25 kV).

III DATA ANALYSIS

A - HEAVY RESIDUES : evaporation residues ?

Results from singles measurements in the TOF telescope will first be examined. Fig. 1 presents mass-velocity diagrams measured at 6° for the two systems studied. For the Ho target, the contribution from the Al backing has been subtracted. Both exhibit the same gross features : a bulk of heavy residues, centered at a mass value smaller than the target mass by about 20 u, and at a velocity somewhat lower than that of the center-of-mass. On the light mass side the lower velocity part of the light fragment spectrum is visible[28], as only those nuclei which stop in the solid state detector have been displayed in these figures.

Finally between these two groups, a third one is visible, more clearly for the Ar + Ho reaction than for the Ar + Ag one, which will be attributed to fission fragments (see next subsection).

Can the heavy residues be called "*evaporation residues*"? To answer this question, a closer examination of their characteristics is needed. For this purpose the residue zones have been divided into four bins of 11-12 u, for which the velocity spectra were analyzed.

Indeed, if one is dealing with evaporation residues of fusion nuclei, having emitted particles isotropically in space, their velocity distribution in the fusion nuclei reference frame is Maxwellian : $d^2\sigma/d\bar{\Omega}d\bar{v} \propto v^2 \exp(-\bar{v}^2/2s^2)$. After transformation into the lab. system the residue velocity spectra at the lab. angle θ become : $d^2\sigma/d\Omega dv \propto v^2 \exp(-v_r^2 \sin^2\theta/2s^2) \exp -((v-v_r \cos\theta)^2/2s^2)$, where v_r is the recoil velocity of the fusion nuclei in the lab. Therefore the Lorentz-invariant distribution $v^{-2}d^2\sigma/d\Omega dv$ is a gaussian, centered at the value $v_r \cos\theta$.

For the mass bins defined above, the invariant velocity spectra measured at five angles are displayed in fig. 2. In all cases, except the highest mass bin, the velocity spectra are reasonably well fitted by gaussian distributions. The position $< v >$ of the maximum is shifted towards lower velocities :

i) at one angle when the mass of the residues is increased. The shift remains however rather small for the three lower bins, and increases suddenly for the highest one of each system. This and the non-gaussian shape of the spectra suggest a strong contribution from peripheral collisions (i.e. low recoil velocities) in the production of these nuclei whose masses are close to the target mass. Therefore they will not be considered in the following analysis. Besides, our experimental threshold ($\sim$ 0.5 cm/ns) prevents the observation of most peripheral collision residues.

ii) for a given mass bin when the detection angle is increased. More precisely it follows the cosine of this angle, as shown in fig. 3, where the values $< v >/(v_{FMT} \cos\theta)$ appear nearly constant versus θ. It should be noted that for the system Ar + Ho, at 50°, the maximum could not be observed because of the experimental velocity threshold.

The shape of the velocity spectra and the variation of their maximum versus θ are first clues that the observed heavy residues may be evaporation residues. It follows from fig. 3 that the average recoil velocity of the fusion-like nuclei, from which the measured residues originate, increases when the mass of the residues decreases. As will be stated later, this means that the lower measured masses are preferentially associated with the largest LMT, and consequently with the largest mass and excitation energy transfers. The influence of the growing number of evaporated particles appears as an increase in the width of the velocity spectra when the residue mass decreases.

A confirmation of this influence is given by the examination of angular distributions, plotted as $d\sigma/d\theta$, for the different mass bins (fig. 4). First, the positions of the maxima around 10 - 15°, despite the high recoil velocities, indicate an important evaporation effect. A closer inspection shows that this maximum is shifted towards larger angles when the residue mass decreases, as can be expected if more particles are evaporated.

In summary, the characteristics of the angular and velocity distributions of these heavy residues are strong arguments that they are evaporation residues from fusion-like nuclei.

B - FISSION

To search for binary fission events, a coincidence between the TOF telescope and the PPAC was required. The coincidence requirement selects in the mass-velocity space the intermediate zone between heavy residues and light fragments, which appears clearly in fig. 1 for the Ar + Ho system. Fission events were more precisely selected by imposing gates on the mass and velocity of fragments detected in the TOF telescope, and also on the relative velocity of the coincident fragments. The final result appears in fig. 5, which is a diagram of the number of events in a mass (TOF)-correlation angle plane. All the selected events lie in a zone delimited by lines representing calculated correlations[29], assuming binary fission after LMT equal to 1 to 0.6 times projectile momentum, and the same energy removed per nucleon as deduced from the residue data (see sect. V.A). This is a clear signature of fission following a fusion-like process.

IV FUSION-LIKE PROCESS CHARACTERISTICS

A - LINEAR MOMENTUM TRANSFER

From their recoil velocity, one can derive the linear momentum transferred to the fusion-like nuclei. We have performed this calculation assuming an incomplete fusion mechanism : only a fraction of the projectile nucleons fuses with the target, the remaining nucleons being ejected close to 0° with the beam velocity. The linear momentum, p, transferred to the fusion-like nuclei with recoil velocity v_r is then related to the projectile momentum p_i by the relation :

$$p = p_i \frac{m_t}{m_p} \frac{v_r}{v_p - v_r} \qquad (1)$$

where the subscripts p and t refer to projectile and target. For evaporation residues, the calculation has been performed for the whole zone delimited by the dashed lines in fig. 1. The most probable values are (0.64 ± 0.06) p_i for Ar + Ag, and (0.74 ± 0.03) p_i for Ar + Ho. One observes a rather large difference between the two systems, which will be discussed later.

For fission, the projection of figure 5 on the $(\theta_1 + \theta_2)$ axis gives the angular correlation distributions (fig. 6) as they are generally presented for fissile systems[21]. In figure 6, the momentum scale is deduced from the angular scale by assuming symmetric splitting. The most probable LMT for fusion-fission events, deduced from the recoil velocity at the maximum of the correlation, are about 0.9 p_i for Ar + Ag and 0.8 p_i for Ar + Ho. But it is evident from fig. 5 that the mass distribution of fission fragments introduces a much larger spread in the correlation angle when the lighter fragment rather than the heavy one is detected in the TOF telescope. To get more precise results, the measured mass asymmetry of fission fragments was used to calculate, event by event, the recoil velocity of the fissioning nuclei. Further assumptions are required, namely that the fissioning nucleus flies in the beam direction, and that evaporation does not modify the mass asymmetry significantly. The first assumption is reasonable in view of experimental results[15,16] which show that the width of the recoil angle distribution of fissioning nuclei is about 10°, for central collisions. The second assumption requires the sharing of excitation energy proportional to fragment masses. If R is the ratio M_1/M_2, fragment one being detected in the TOF telescope, then

$$v_r = \frac{v_1}{1+R} (\sin \theta_1 \tan (\pi/2 - \theta_2) + \cos \theta_1) \qquad (2)$$

One therefore obtains a recoil velocity spectrum at zero degrees, which is plotted in fig. 7 and compared with the residue velocity spectrum measured at 6°.

It appears that, for the Ar + Ho system, the residue and fission spectra are rather similar both in position and shape ; only a slightly higher mean velocity is obtained for the fissioning nuclei, together with a smaller width. Conversely, the residue and fission spectra for the Ar + Ag system are very different : the latter has a much higher mean velocity, and its width is significantly smaller. This large difference indicates that the deexcitation phase introduces a selection in LMT for this system. This will be discussed in section V. The values of most probable LMT are summarized in table 1. Finally, one can also note that the most probable LMT for fissioning nuclei derived from the velocity spectra is somewhat lower than that deduced from the maximum of the angular correlation for the Ar + Ag system (0.8 p_i compared to 0.9 p_i), while it is roughly the same for the Ar + Ho system (about 0.8 p_i). The difference gives an idea on the error introduced by the symmetric splitting approximation ; it is not negligible for the lightest system considered here.

B) CROSS-SECTIONS

Fusion - like cross-sections for the two systems have been derived by summing evaporation residue and fission cross sections (table 1). The former were obtained by integration of the angular

distributions (fig. 4), while the latter were derived assuming angular distributions proportional to 1/sinθ in the fissioning nuclei frame. The ratio of fission and evaporation residue cross-sections reflects fission-evaporation competition, which will be discussed in next section.

Fusion cross-sections measured here are much smaller than those measured at 8.5 MeV per nucleon, which amount to about 1250 mb in both cases[30-32]. Therefore one observes a strong decrease of the fusion-like cross-section when the bombarding energy is increased. Actually this decrease is expected to start around 8 MeV per nucleon, due to the existence of an angular momentum limit to fusion which arises from friction forces[33]. Moreover, the weakening of mean field effects with increasing energy should also lead to a decrease of fusion cross-sections. If one assumes that fusion-like reactions occur for the most central collisions, with a sharp ℓ cut-off, the initial partial waves leading to these reactions can be deduced from the fusion cross-sections. Although it might be a mere chance, it is interesting to note that the maximum ℓ for fusion "ℓ_{fus}" found at 27 MeV per nucleon is very close to the Bass ℓ_{lim}[33] for both systems (120 $\hbar$ for Ar + Ag and 137 $\hbar$ for Ar + Ho). In fig. 8 the ratio ℓ_{fus}/ℓ_{max} is displayed versus the incident energy for the two systems studied. The behavior of this ratio is the same for the two reactions ; the percentage of initial partial waves leading to fusion-like reactions decreases strongly with increasing bombarding energy, down to about 30 % at 27 MeV per nucleon.

V DEEXCITATION OF HOT NUCLEI

A) EXCITATION ENERGIES

The excitation energies given to the fusion-like nuclei can be calculated in the framework of the incomplete fusion picture :

$$E^* = \frac{m\, m_t\, E_p}{m_p(m + m_t)} + Q \qquad (3)$$

if m nucleons of the projectile fuse with the target. There is a large uncertainty of the value of the mass balance, Q, which depends strongly on whether the projectile nucleons which do not fuse escape as free nucleons or as bound particles. An average value was taken to calculate the excitation energies listed in table II, where the uncertainty of E^* reflects only the uncertainty on Q. The most probable final mass < M > corresponding to a given value of p can be obtained from fig. 1 (dashed - dotted line). Therefore one can derive the average number of nucleons evaporated and the average energy removed per nucleon, ε. Table II summarizes all these calculations. One observes that, if the fusion nucleus mass increases with p, the average final mass varies in the reverse way. This is indeed what is expected if the excitation energy varies as indicated by equation (3), and if the energy removed per nucleon is roughly constant.

The rather low values of the energy removed per nucleon, despite the high temperatures of the fusion-like nuclei (T > 5 MeV), indicate that a large fraction of nucleons are evaporated as clusters (α and possibly heavier fragments). Assuming, as a first approximation, that only neutrons, protons and α particles are evaporated and that the average temperature along the decay chain is equal to 2/3 the initial

temperature[34], one can estimate the relative yield of α particles from the observed values of ε. It is found that half the evaporated nucleons should be bound into α particles for Ar + Ag, and 40 % for Ar + Ho. The neutron to proton ratio was taken equal to 3 (which corresponds to roughly equal numbers of protons and alphas), but any larger value would give the same α yields. Indeed high α multiplicities have been observed experimentally for nuclei with similar excitation energies[35]. By taking into account binary fission kinetic energy, one can calculate in the same way the excitation energy of fission fragments, which is given in the last line of table II ; the average final mass is known experimentally (fig. 9), as well as the most probable LMT. The energy removed per nucleon appears to be very close to that found for evaporation residues, which justifies a posteriori the assumption made in sect. III.3.

When fusion-like nuclei undergo fission, information on their excitation energies can be derived from the width of the out-of-plane distribution of fission fragments. These distributions are displayed in fig. 10, and their widths listed in table III. At such excitation energies the variance of the distribution can be well approximated by the expression :

$$\sigma^2 \simeq \Sigma\, 1/p_F^2 \, < E > n \, (1 + n/M) \qquad (4)$$

where :

$< E >$ is the average kinetic energy of evaporated particles : ($< E > = B + 4/3\ T$), B being the barrier to evaporation

n is the total number of nucleons removed by these particles, from a total initial mass equal to M ;

P_F is the average momentum of the fission fragments.

The summation is over all types of particles, but we have considered only p, n and α. Their relative yields were derived as explained before. The value of the initial temperatures of fissioning nuclei thus derived are indicated as T_1 in table III. Expression (4), however, is valid if all particles are evaporated by the fission fragments. It has been known for some years that some of them are evaporated by the fusion nuclei prior to fission[36-38]. In the extreme - and unrealistic - case where all particles would be emitted prior to fission, the width would be given by an equation similar to (4), with the impulse of the fusion nucleus replacing that of the fission fragment. Temperatures so calculated are listed as T_2 in table III, and realistic temperatures can be found in between T_1 and T_2, in agreement with what can be deduced from the excitation energies.

Residue, as well as fission characteristics indicate that the simple reaction scheme used all along gives a rather good estimate of the physical quantities involved in the reactions studied here. Particularly one has confidence that the calculated values of the excitation energies are quite realistic. The most probable excitation energy of fusion-like nuclei is about 500-600 MeV for both systems, and the distribution extends up to more than 700 MeV ; this indicates that nuclei have been formed in extreme conditions, close to the limit of instability.

B) DEEXCITATION : FISSION-EVAPORATION COMPETITION

Having formed such hot nuclei, one can wonder how they will deexcite. Both evaporation residues and fission fragments have been observed as cold remnants of these hot fusion nuclei, which gives

the capability of studying the fission-evaporation competition at very high excitation energy.

The evolution of the ratio $\sigma_{ER}/(\sigma_{ER} + \sigma_{FISS})$ with incident energy is displayed in fig. 11. For both systems, a change of the slope is observed when the bombarding energy reaches 8-9 MeV per nucleon, indicating inhibition of the fission path in favor of the evaporation path. Two reasons can be found to explain this evolution. Firstly, as was stated in the introduction, the onset of incomplete fusion occurs in this energy region, lowering masses and atomic numbers of fusion-like nuclei and therefore their fission probability. The second reason can be found in the deexcitation process itself and will be examined more closely.

Since the pioneer work of Alexander et al.[26,36] and from more recent studies[37,38] we know that prefission evaporation occurs when temperatures larger than about 3 MeV are reached. This evaporation is now well understood, at least qualitatively, in terms of particle emission time and fission time[39,40]. To reach the saddle point, times as long as a few 10^{-21} s are needed[41] and these times become, with increasing excitation energies, of the order of or larger than particle emission times. Therefore the fission channel is fully open only when fusion-like nuclei have already lost a non-negligible part of their excitation energy, and several mass and atomic number units ; this dynamical effect probably overcomes the decrease of fission barriers due to high temperatures[42,43] and angular momenta, so that globally the fission probability decreases.

Let us come now to the observations made here at very high excitation energies (table I), and consider first the Ar + Ho sys-

tem. Very close average LMT have been found for all fusion-like nuclei, whether they subsequently undergo fission or give birth to evaporation residues. This is a signature that the deexcitation phase does not introduce any selection in the population of fusion-like nuclei resulting of the preequilibrium stage. This is possible only if the role of the fission barrier is negligible, at least at the beginning of the deexcitation. For the zone of nuclei reached in the Ar + Ho reaction, the evolution of the fission barrier with temperature and angular momentum is qualitatively given in fig. 12.a[44]. It follows that, whatever the LMT, the initial excitation energy is high enough to annihilate the fission barrier. The large observed proportion of residues can nevertheless be explained by prefission evaporation ; for example for an excitation energy of 200 MeV, the fraction of residues observed for Ar + $^{154}_{62}Sm$ is three times that measured for Ar + $^{164}_{66}Dy$[26]. The angular momentum distribution, very difficult to estimate properly, can be assumed to be similar over all the fusion-like nuclei population[45]. It turns out, therefore, that the Ar + Ho reactions at 27 MeV per nucleon produce an ensemble of fusion-like nuclei well suited for fission-evaporation competition calculations.

Fusion-like nuclei from the Ar + Ag system behave very differently ; it appears that the average LMT values corresponding to fission and residues are far apart ; unlike the Ar + Ho system, deexcitation introduces a selection in the fusion-like nuclei population. It is well known that fissility strongly decreases in the region of the nuclei produced here and therefore fission is really competitive only for the heaviest nuclei, i.e. those produced through the largest LMT.

Moreover, fig. 12.b shows that for this zone of nuclei[46] the effect of angular momentum is now predominant.

Finally it can be emphasized that if multiplicity studies of particles evaporated prior to fission give direct information about fission-evaporation competition at the beginning of the deexcitation, residue and fission cross-sections reflect the competition over the whole chain ; therefore they can be used for more quantitative comparisons with calculations.

VI INFLUENCE OF HEAVY CLUSTER EVAPORATION ON VELOCITY AND ANGULAR DISTRIBUTION

It was noticed in sect. III that residue angular distributions were broad and extended up to large angles. One generally expects evaporation residues to be focused in a narrow cone around the beam direction, even at high energy, as the large recoil velocity nearly compensates for an increased number of evaporated particles. Broader angular distributions would be expected, however, if heavy cluster evaporation becomes non-negligible. Such evaporation has been shown to occur in 30 MeV/nucleon ^{3}He induced reactions in Ag targets, but with low probability[47].

In the case of the Ar + Ag reaction studied here, inclusive data on heavy clusters (Z = 3 to 11) have been obtained[28]. By studying their energy spectra between 6 and 50°, the heavy clusters were found to originate from three sources, one of which having a velocity close to the average residue velocity. Therefore it appears reasonable to test the influence of cluster evaporation on residue characteristics, as the ratio of cluster to residue cross-section is about 2:1[24].

For this purpose Monte-Carlo simulations were performed with the help of a modified version of the code LINDA[48]. Only residues were studied, no fission competition was included. LMT distribution was simulated by emission of "direct" particles, with a gaussian velocity distribution in the projectile reference frame. The average number of direct nucleons was 14.4 (< LMT > = 0.64), chosen as 3.2 neutrons, 3.2 protons and 2 α, with a standard deviation equal to 2.15.

Fusion-like nuclei formed after this first step deexcite through particle evaporation. Relative emission widths for light particles (n, ^{1,2,3}H and ^{3,4}He) were calculated at each step, by means of the formalism of Friedman and Lynch[49]. Heavy cluster evaporation was introduced in the following way : for each event, 2 or 3 clusters (2.1 on the average, with probabilities proportional to their relative cross-sections) were emitted at the beginning of the evaporation chain.

The possibility that clusters may be emitted in excited states was taken into account by a proper modification of their binding energy[49]. The remaining excitation energy was then dissipated through light particle emission as before. Two simulations were performed, with and without cluster evaporation. The average final mass is well reproduced by the calculation, but the width of the calculated mass distribution is about half the experimental width : this may come partly from the experimental resolution.

The velocity distribution (fig. 13) and the calculated spectrum agree rather well when heavy clusters are evaporated. The most interesting effect of heavy cluster evaporation appears on angular distributions. It increases significantly both the position of the maximum

and the width, and introduces a tail at large angles. However these effects are not sufficient to reproduce the experimental distributions. One should keep in mind that in the calculated "preequilibrium step", only light particles ($Z < 2$) with the beam velocity have been considered. If some heavier clusters are emitted during this step with velocities equal to or lower than the beam velocity,an increased transverse momentum would be given to the fusion-like nuclei, broadening the angular distribution of residues. Experiments where these heavy clusters would be detected in coincidence with residues are now necessary to clarify this point. We think nevertheless that the inclusive data presented in this paper do support a rather large cluster evaporation probability.

SUMMARY

Through inclusive measurements of nuclei formed in 27 MeV/nucleon Ar induced reactions in Ag and Ho, it is shown that fusion-like reactions still occur at this intermediate energy ; they account for 15 % of the reaction cross-section. Fusion-like nuclei have been characterized through the properties of their cold remnants, either evaporation residues or fission fragments. All these properties show that fusion-like nuclei were formed with a very high excitation energy, close do the limits predicted by different theoretical models. Cross-section fractionation between ER and fission shows that fission barriers still play an important role, even at high excitation energy, due to the very short particle emission time as compared to fission time. Finally the broad residue angular distributions observed could be partly explained by a sizeable evaporation of heavy clusters.

We wish to thank the GANIL operating crew, the computer staff, and J.L. CIFFRE for their support during the experiment. We are grateful to G. PEASLEE for careful reading of the manuscript.

REFERENCES

1 - M. LEFORT and C. NGO, Ann. Phys. 3, 5 (1978).

2 - R. BASS, Nuclear Reactions with Heavy Ions, Springer Verlag, Heildeberg (1980).

3 - R. WEINER and M. WESTROM, Nucl. Phys. A286, 282 (1977)

4 - H.S. KOHLER, Nucl. Phys. A378, 159 (1982).

5 - J.P. BONDORF,J.N. DE, A.O.T. KARVINEN, G. FAI and B. JAKOBSSON, Phys. Lett. 848, 162 (1979).

6 - J.P. BONDORF, J.N. DE, G. FAI, A.O.T. KARVINEN, B. JAKOBSSON and J. RANDRUP, Nucl. Phys. A333, 285 (1980).

7 - K. MOHRING, W.J. SWIATECKI and M. ZIELINSKA-PFABE, Nucl. Phys. A440, 89 (1985).

8 - G.D. HARP and J.M. MILLER, Phys. Rev. C3, 1847 (1971).

9 - M. BLANN, Phys. Rev. C31, 1245 (1985).

10 - F. SEBILLE and B. REMAUD, Z. Phys. A310, 99 (1983) and Nucl. Phys. A420, 141 (1984).

11 - S. LERAY, G. LA RANA, C. NGO, M. BARRANCO, M. PI and A. VINAS, Z. Phys. A320, 383 (1985).

12 - V.E. VIOLA, Jr., B.B. BACK, K.L. WOLF, T.C. AWES, C.K. GELBKE and H. BREUER, Phys. Rev. C26, 178 (1982).

13 - M.F. RIVET and B. BORDERIE, report IPNO-DRE-84-32 (1984) and Proc. of the Tsukuba Int. Symp. on H.I. Fusion Reaction, World Scientific, 311 .

14 - J. GALIN, H. OESCHLER, S. SONG, B. BORDERIE, M.F. RIVET, I. FOREST, R. BIMBOT, D. GARDES, B. GATTY, H. GUILLEMOT, M. LEFORT, B. TAMAIN and X. TARRAGO, Phys. Rev. Lett. 48, 1787 (1982).

15 - E.C. POLLACO, M. CONJEAUD, S. HARAR, C. VOLANT, Y. CASSAGNOU, R. DAYRAS, R. LEGRAIN, M.S. NGUYEN, H. OESCHLER and F. SAINT LAURENT, Phys. Lett. 146B, 29. (1984).

16 - C. VOLANT, Proc. XXIII Int. Wint. Meeting on Nucl. Phys. Bormio (1985), 370.

17 - B. BORDERIE and M.F. RIVET, Z. Phys. A321, 703 (1985)

18 - G. AUGER, D. JOUAN, E. PLAGNOL, F. POUGHEON, F. NAULIN, H. DOUBRE and C. GREGOIRE, Z. Phys. A321, 243 (1985) D. JOUAN, Thesis, Orsay (1985).

19 - F. RAMI, J.P. COFFIN, G. GUILLAUME, B. HEUSCH, P. WAGNER, A. FAHLI and P. FINTZ, Nucl. Phys. A444, 325 (1985).

20 - J. BLACHOT, J. CRANCON, B. DE GONCOURT, A. GIZON, A. LLERES and H. NIFENECKER, Proc. XXIII Int. Wint. Meeting on Nucl. Phys., Bormio (1985).

21 - D. JACQUET, E. DUEK, J.M. ALEXANDER, B. BORDERIE, J. GALIN, D. GARDES, D. GUERREAU, M. LEFORT, F. MONNET, M.F. RIVET and X. TARRAGO, Phys. Rev. Lett. 53, 2226 (1984).

22 - P. BONCHE, S. LEVIT and D. VAUTHERIN, Nucl. Phys. A427, 278 (1984) and Nucl. Phys. A436, 265 (1985).

23 - S. LEVIT and P. BONCHE, Nucl. Phys. A437, 426 (1985).

24 - B. BORDERIE, XVII Masurian School on Nuclear Physics, Mikolajki, 1985, IPNO DRE 85.23.

25 - J.P. BONDORF, R. DONANGELO, H. SCHULZ, K. SNEPPEN, Phys. Lett. 162B, 30 (1985).

26 - D. LOGAN, H. DELAGRANGE, M.F. RIVET, M. RAJAGOPALAN, J.M. ALEXANDER, M. KAPLAN, M.S. ZISMAN and E. DUEK, Phys. Rev. C22, 1080 (1980).

27 - B. BORDERIE, M.F. RIVET, C. CABOT, D. FABRIS, D. GARDES, H. GAUVIN, F. HANAPPE and J. PETER, Z. Phys. A316, 243 (1984).

28 - B. BORDERIE, M.F. RIVET, C. CABOT, D. FABRIS, D. GARDES, H. GAUVIN, F. HANAPPE and J. PETER, Z. Phys. A318, 315 (1984).

29 - V.E. VIOLA, K. KWIATKOWSKI and M. WALKER, Phys. Rev. C31, 1550 (1985).

30 - H.C. BRITT, B.H. ERKKILA, R.H. STOKES, H.H. GUTBROD, F. PLASIL, R.L. FERGUSON and M. BLANN, Phys. Rev. C13, 1483 (1976).

31 - L.C. VAZ, D. LOGAN, J.M. ALEXANDER, E. DUEK, D. GUERREAU, L. KOWALSKI, M.F. RIVET and M.S. ZISMAN, Z. Phys. A311, 89 (1983).

32 - B. BORDERIE, M. BERIANGER, D. GARDES, F. HANAPPE, L. NOWICKI, J. PETER, B. TAMAIN, S AGARWALL, J. GIRARD, C. GREGOIRE, J. MATUSZEK and C. NGO, Z. Phys. A299, 263 (1981).

33 - R. BASS, Nucl. Phys. A231, 45 (1974).

34 - T. DOSSING and J. RANDRUP, Nucl. Phys. A433, 280 (1985).

35 - A. GOBBI, Proceedings of the XXIII International Winter Meeting on Nuclear Physics, Bormio (1985) p. 569.

36 - M.F. RIVET, D. LOGAN, J.M. ALEXANDER, D. GUERREAU, E. DUEK, M. ZISMAN and M. KAPLAN, Phys. Rev. C25, 2430 (1982).

37 - S. SONG, M.F. RIVET, R. BIMBOT, B. BORDERIE, I. FOREST, J. GALIN, D. GARDES, B. GATTY, M. LEFORT, H. OESCHLER, B. TAMAIN and X. TARRAGO, Phys. Lett. 130B, 14 (1983).

38 - D. JACQUET, J. GALIN, B. BORDERIE, D. GARDES, D. GUERREAU, M. LEFORT, F. MONNET, M.F. RIVET, X. TARRAGO, E. DUEK and J.M. ALEXANDER, Phys. Rev. C32, 1594 (1985).

39 - S. HASSANI and P. GRANGE, Phys. Lett. 137B, 281 (1984) and P. GRANGE, Nucl. Phys. A428, 37c (1984).

40 - H. DELAGRANGE, C. GREGOIRE, F. SCHEUTER and Y. ABE, Ganil report 85-07 (1985).

41 - J.R. NIX and A.J. SIERK Preprint LA-UR-84-4008.

42 - X. CAMPI, S. STRINGARI, Z. Phys. A309. 239 (1983).

43 - B. BARTEL and Ph. QUENTIN, Phys. Lett. 152B, 29 (1985).

44 - D. DALILI, J. NEMETH and C. NGO, Z. Phys. A321, 335 (1985).

45 - M.N. NAMBOODIRI, R.K. CHOUDHURY, L. ADLER, J.D. BRONSON, D. FABRIS, U. GARG, P.L. GONTHIER, K. HAGEL, D.R. HAENNI, Y.W. LUI, Z. MAJKA, G. MOUCHATY, T. MURAKAMI, J.B. NATOWITZ, G. NEBBIA, R.P. SCHMITT, S. SIMON, J.P. SULLIVAN and D.H. YOUNGBLOOD, Preprint (1985).

46 - J. NEMETH, D. DALILI and C. NGO, Phys. Lett. 154B (1985) 11.

47 - L.G. SOBOTKA, M.L. PADGETT, G.J. WOZNIAK, G. GUARINO, A.J. PACHECO, L.G. MORETTO, Y. CHAN, R.G. STOKSTAD, I. TSERRUYA and S. WALD, Phys. Rev. Lett. 51, 2187 (1983).

48 - E. DUEK, L. KOWALSKI and J.M. ALEXANDER, Computer Physics Communications 34, 395 (1985).

49 - W.A. FRIEDMAN and W.G. LYNCH, Phys. Rev. C28, 16 (1983).

TABLE 1

	RESIDUES		FISSION		FUSION		
	σ(mb)	p/p_i	σ(mb)	p/p_i	σ(mb)	p/p_i	"ℓ_{fus}" $\hbar$
Ar + Ag	290 ± 45	0.64 ± 0.06	160 ± 30	0.80 ± 0.06	450 ± 75	0.70 ± 0.06	126 ± 11
Ar + Ho	160 ± 25	0.74 ± 0.03	400 ± 50	0.78 ± 0.08	560 ± 75	0.77 ± 0.05	155 ± 10

TABLE 2

	Ar + Ag					Ar + Ho				
p/p_i	$m + m_t$	$< M >$	n_{evap}	E^*	ϵ	$m + m_t$	$< M >$	n_{evap}	E^*	ϵ
0.95	146	84 ± 2	62	704 ± 1	11.3 ± 0.4	203	140 ± 2	63	745 ± 1	11.8 ± 0.4
0.85	142	86 ± 2	56	630 ± 15	11.2 ± 0.7	199	143 ± 2	56	663 ± 15	11.8 ± 0.7
0.75	138	88 ± 2	50	551 ± 30	11.0 ± 1.1	195	146 ± 2	49	576 ± 30	11.8 ± 1.1
0.65	134	91 ± 2	43	468 ± 45	10.9 ± 1.5	191	150 ± 2	41	484 ± 45	11.8 ± 1.7
0.55	130	93 ± 2	37	381 ± 60	10.3 ± 2.1	187	153 2	34	390 ± 55	11.5 ± 2.3
0.80	140	88	52	564	10.9	197	144	53	619	11.7

TABLE 3

	FWHM	All evaporation from F.F T_1	All evaporation before fission T_2	$\sqrt{8E^*/A}$
Ar + Ag	20 ± 1°	4.0 ± 0.7	7.6 ± 1.3	5.7
Ar + Ho	17 ± 1°	3.1 ± 0.6	6.0 ± 1.3	5.0

FIGURE CAPTIONS

Figure 1 : Mass velocity spectra of the products measured at 6° for Ar + Ag and Ar + Ho. The arrows indicate full momentum transfer (FMT) velocities. Dashed lines delimit the zones of products identified as evaporation residues. Dashed-dotted lines join the most probable masses for each velocity.

Figure 2 : Velocity spectra measured at different angles for given mass bins of heavy residues. The lines correspond to gaussian fits except for the heavier mass bin of each system, and all 50° data for Ar + Ho.

Figure 3 : Evolution of the most probable velocity, divided by FMT velocity, with the detection angle.

Figure 4 : Angular distributions of evaporation residues.

Figure 5 : Correlation between the measured mass of one fission fragment and the correlation angle $\theta_1 + \theta_2$. The size of the points is proportional to the number of counts. Solid lines represent the expected correlations for binary fission following LMT equal to 100 %, 80 % and 60 % (see text). Crosses on these lines correspond to symmetric splitting.

Figure 6 : Angular correlation distributions of fission fragments, integrated over out-of-plane angles ; circles and triangles correspond to two positions of the PPAC. Arrows indicate LMT values for symmetric fission.

Figure 7 : Velocity spectra measured close to the beam direction for evaporation residues (black circles) and fissioning nuclei (open circles). Solid lines correspond to gaussian fits, all maxima have been arbitrari ly normalized to 1. Arrows indicate FMT velocities.

Figure 8 : Percentage of initial partial waves leading to fusion-like process as a function of incident energy per nucleon over the barrier. ℓ_{fus} is deduced from σ_{fus} within a sharp cut-off approximation.

Figure 9 : Mass distribution of fission fragments.

Figure 10 : Out of plane distribution of fission fragments, summed over all-in plane correlations.

Figure 11 : Evolution of residue over fusion-like cross-sections with incident energy. Solid lines are drawn as a visual guide through experimental data from ref. 26, 30, 31 and this work.

Figure 12 : Evolution of fission barriers with temperature and angular momentum[44,46]. Only the shapes of the contours are relevant, as absolute values are certainly overestimated.

Figure 13 : Velocity spectra at 6° (top) and angular distribution of evaporation residues from the Ar + Ag reaction. The results of simulations without (dashed lines) and with (solid lines) heavy cluster evaporation are compared with experimental data (points).

TABLE CAPTIONS

Table 1 : Measured cross-sections and most probable LMT for evaporation residues, fusion-fission and fusion-like reactions.

Table 2 : Calculated and measured quantities related to fusion-like process, as a function of LMT : mass of the fusion-like nuclei ($m + m_t$), most probable final mass ($< M >$, from the dashed-dotted lines in fig. 1), number of evaporated nucleons ($n = m + m_t - < M >$), total excitation energy E^* from eq. 3, and average energy removed per nucleon ($\varepsilon = E^*/n$). The last line of the table refers to fusion-fission, $< M >$ being now twice the most probable mass deduced from fig. 9.

Table 3 : Comparison of temperatures of fissioning nuclei extracted from the width of the out-of-plane distributions (see text), and deduced from the excitation energy.

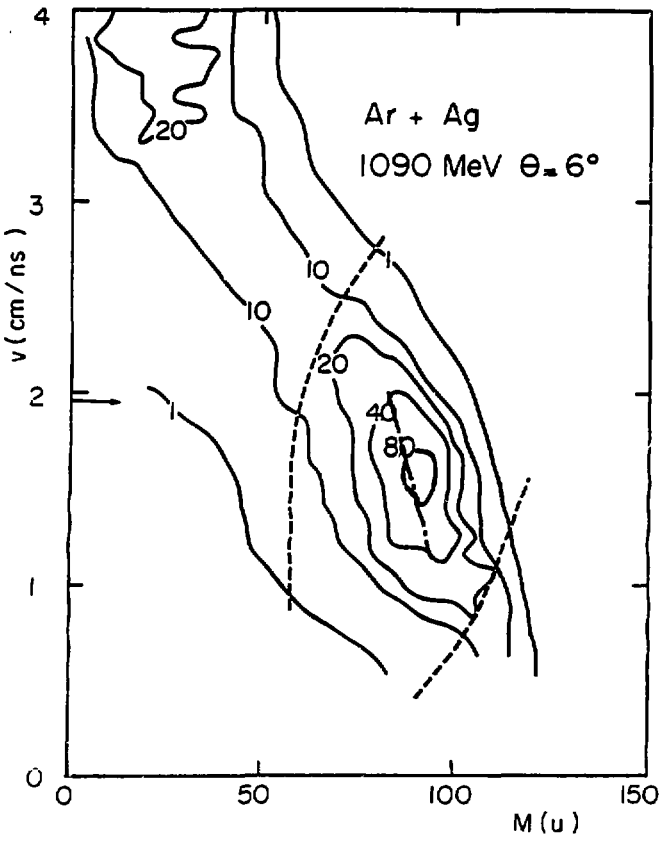

Fig. 1.a

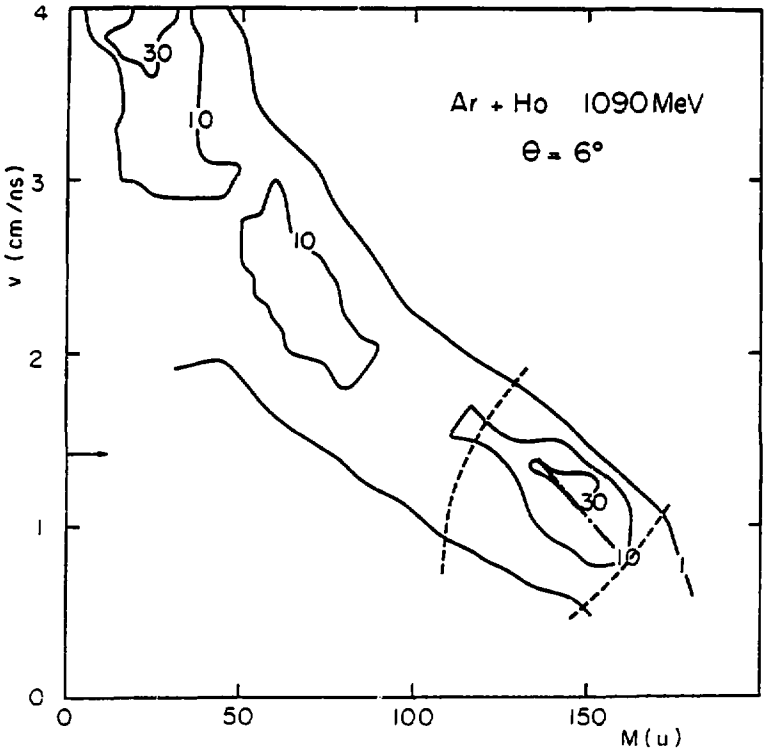

Fig. 1.b

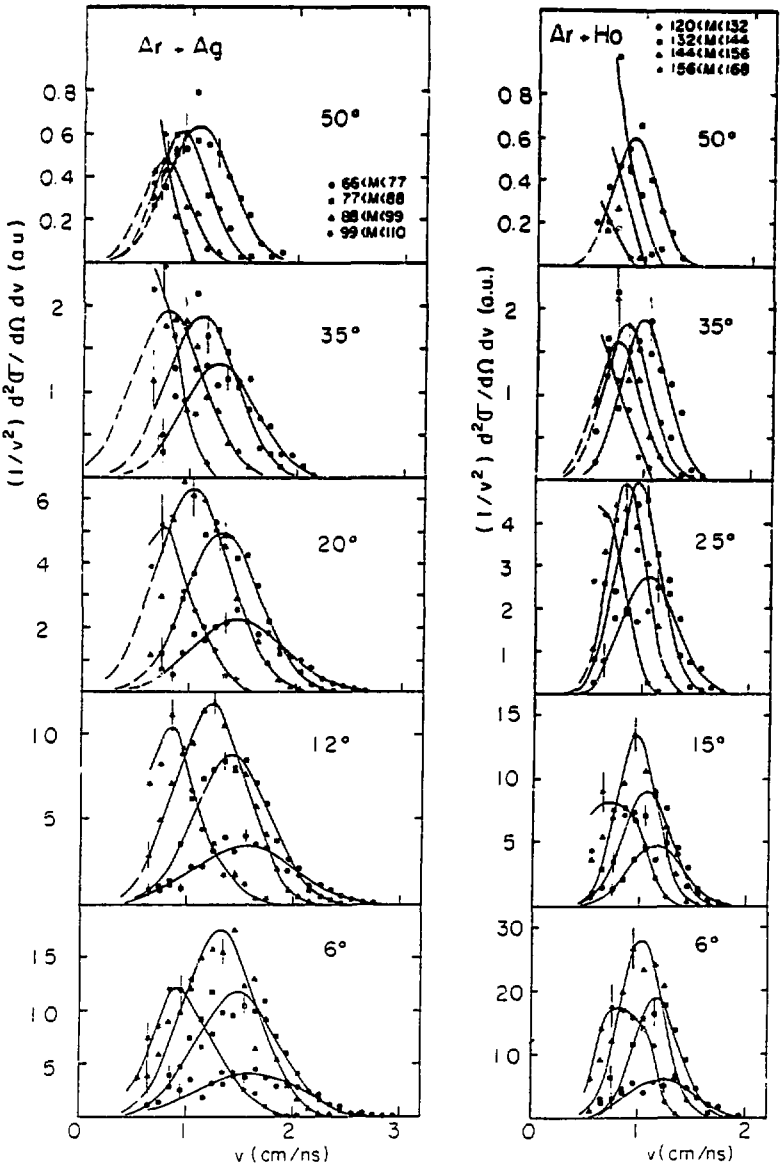
Ar + Ag
50°
35°
20°
12°
6°
66<M<77
77<M<88
88<M<99
99<M<110
(1/v²) d²σ/dΩ dv (a u)
v (cm/ns)
Ar + Ho
120<M<132
132<M<144
144<M<156
156<M<168
25°
15°
(1/v²) d²σ/dΩ dv (a.u.)
v(cm/ns)

Fig. 2

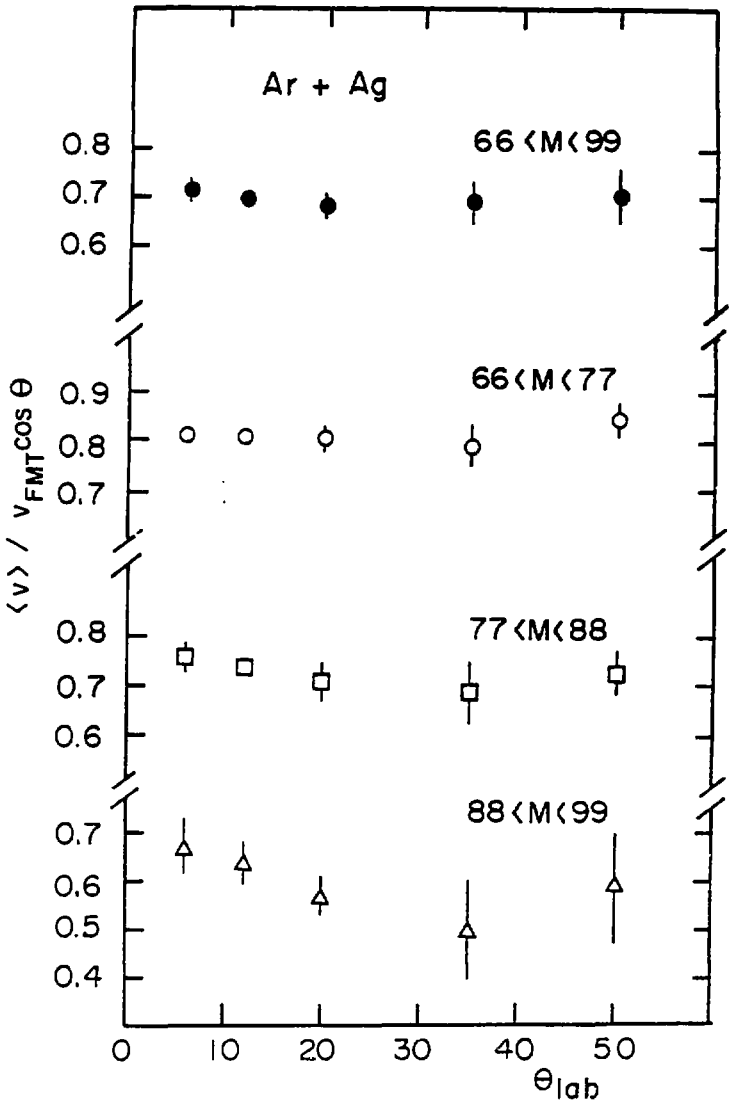
Ar + Ag
66 < M < 99
66 < M < 77
77 < M < 88
88 < M < 99
0.8
0.7
0.6
0.9
0.8
0.7
0.8
0.7
0.6
0.7
0.6
0.5
0.4
0
10
20
30
40
50
θlab
⟨v⟩ / vFMT cos θ

Fig. 3.a

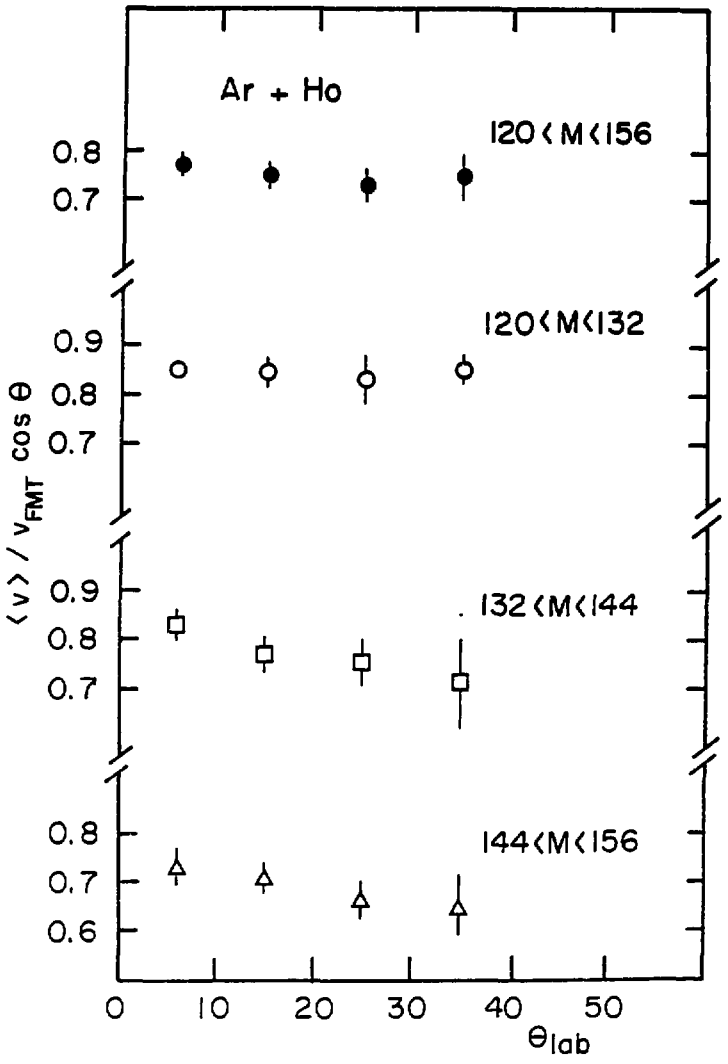
Ar + Ho
120 < M < 156
120 < M < 132
132 < M < 144
144 < M < 156
0.8
0.7
0.9
0.8
0.7
0.9
0.8
0.7
0.8
0.7
0.6
⟨v⟩ / v_FMT cos θ
0
10
20
30
40
50
θlab

Fig. 3.b

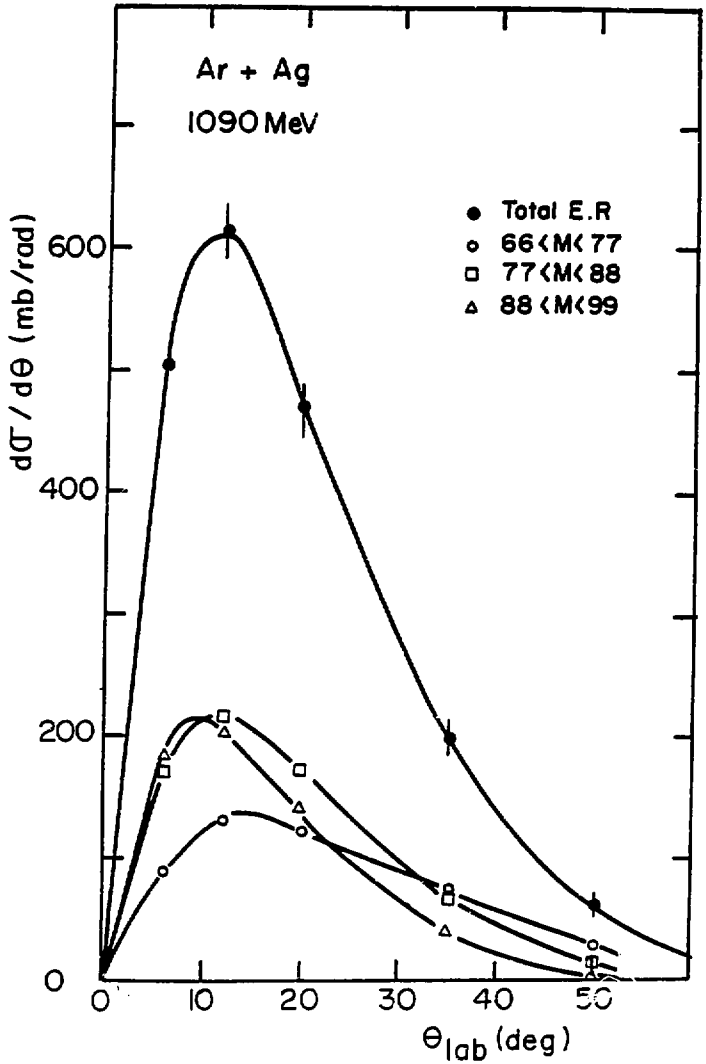
Ar + Ag
1090 MeV
Total E.R
66<M<77
77<M<88
88<M<99
dσ / dθ (mb/rad)
600
400
200
0
0
10
20
30
40
50
θlab (deg)

Fig. 4.a

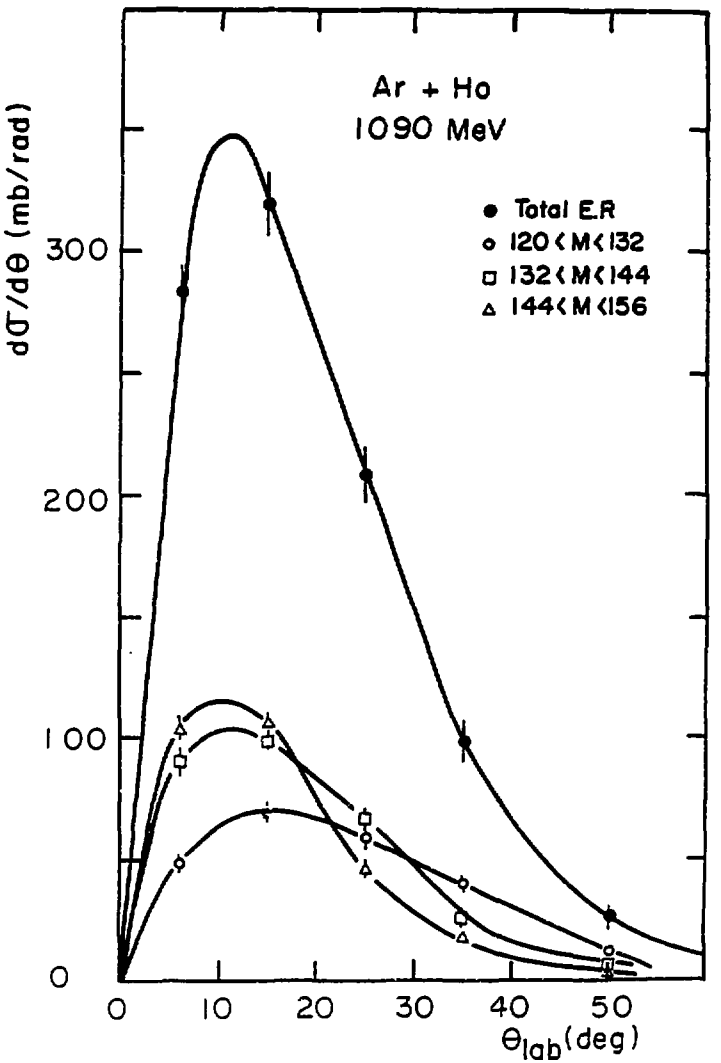
Ar + Ho
1090 MeV
Total E.R
120 < M < 132
132 < M < 144
144 < M < 156
dσ/dθ (mb/rad)
300
200
100
0
0
10
20
30
40
50
θlab (deg)

Fig. 4.b

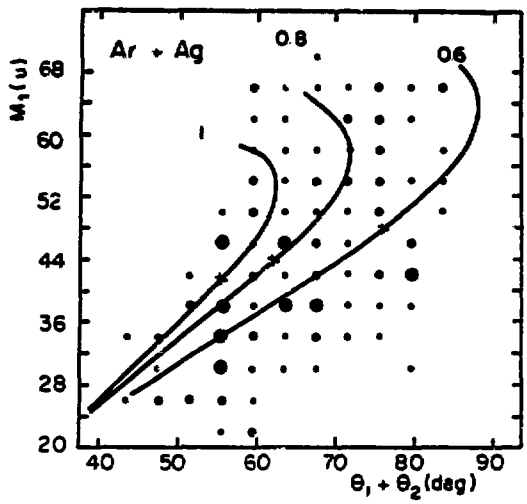
Ar + Ag
0.8
0.6
1
M_1(u)
68
60
52
44
36
28
20
40
50
60
70
80
90
$\theta_1 + \theta_2$(deg)

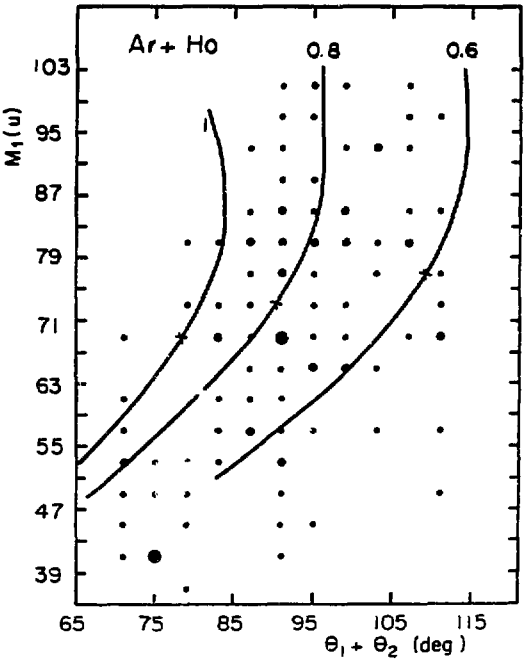
Ar+ Ho
0.8
0.6
1
M_1(u)
103
95
87
79
71
63
55
47
39
65
75
85
95
105
115
$\theta_1 + \theta_2$ (deg)

Fig. 5

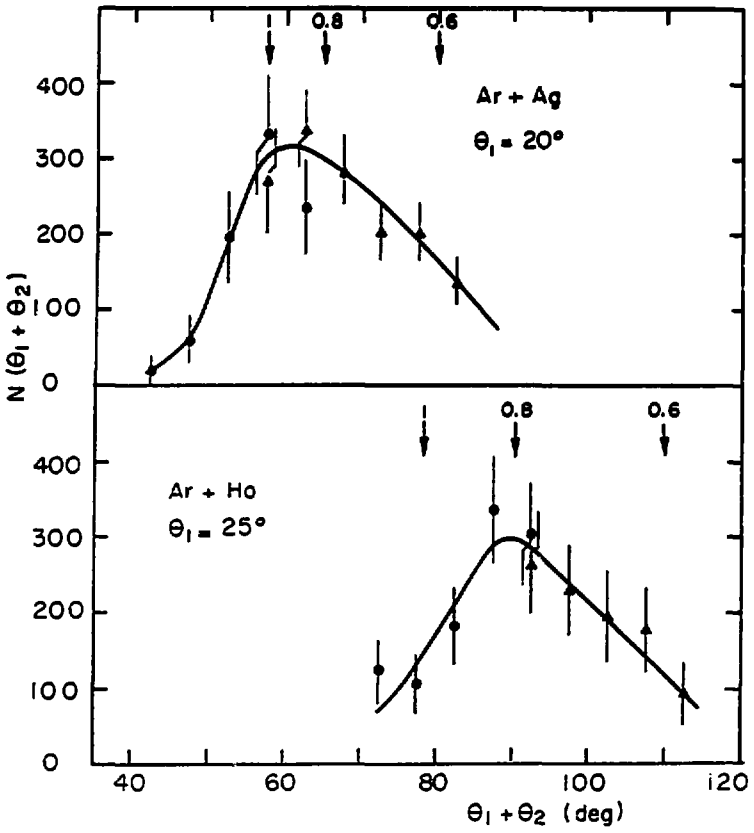
0.8
0.6
Ar + Ag
θ1 = 20°
N (θ1 + θ2)
400
300
200
100
0
0.8
0.6
Ar + Ho
θ1 = 25°
400
300
200
100
0
40
60
80
100
120
θ1 + θ2 (deg)

Fig. 6

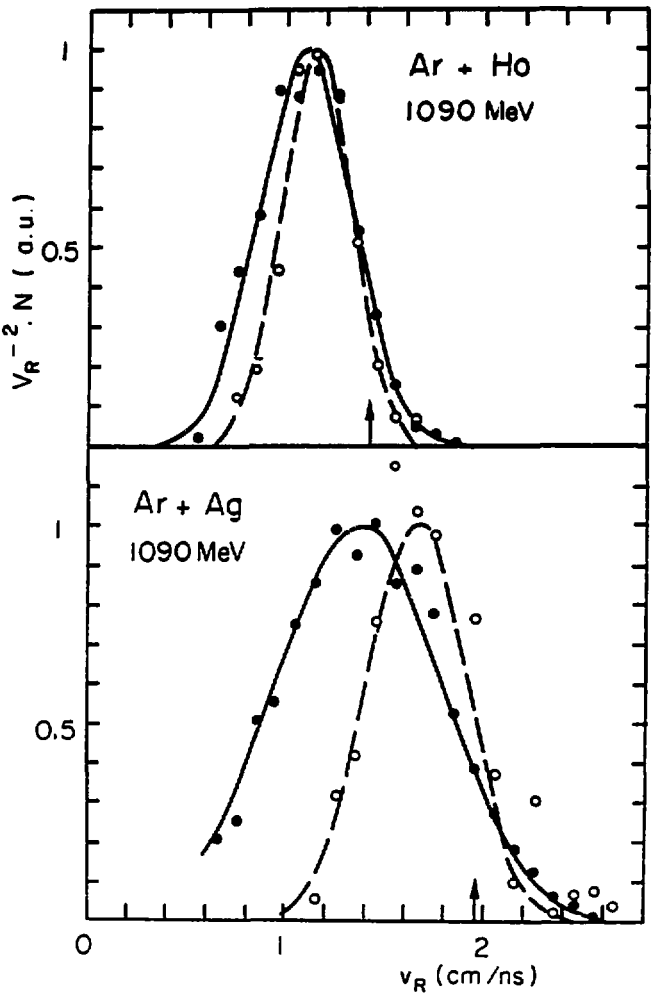

Fig. 7

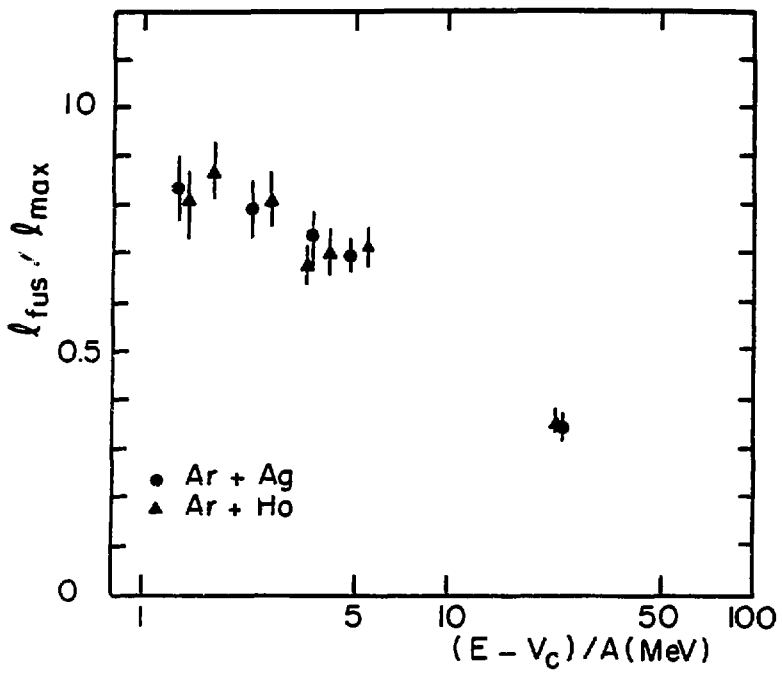

Fig. 8

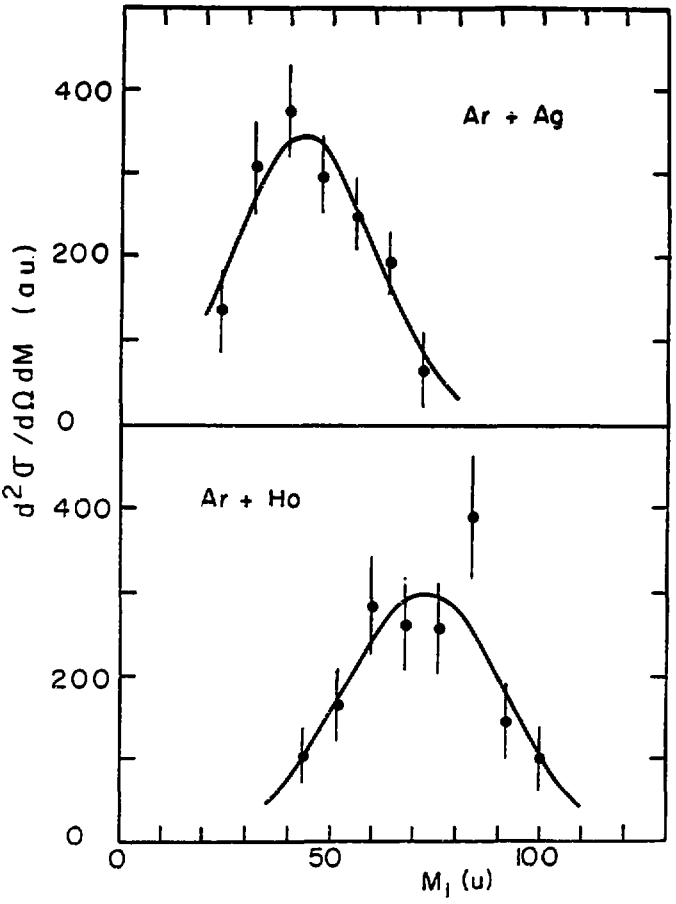

Fig. 9

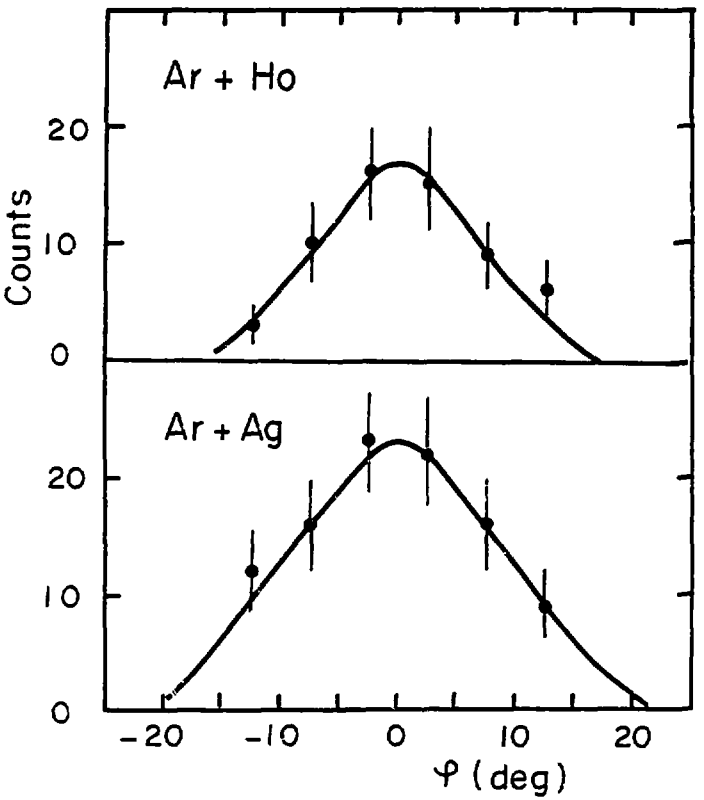

Fig. 10

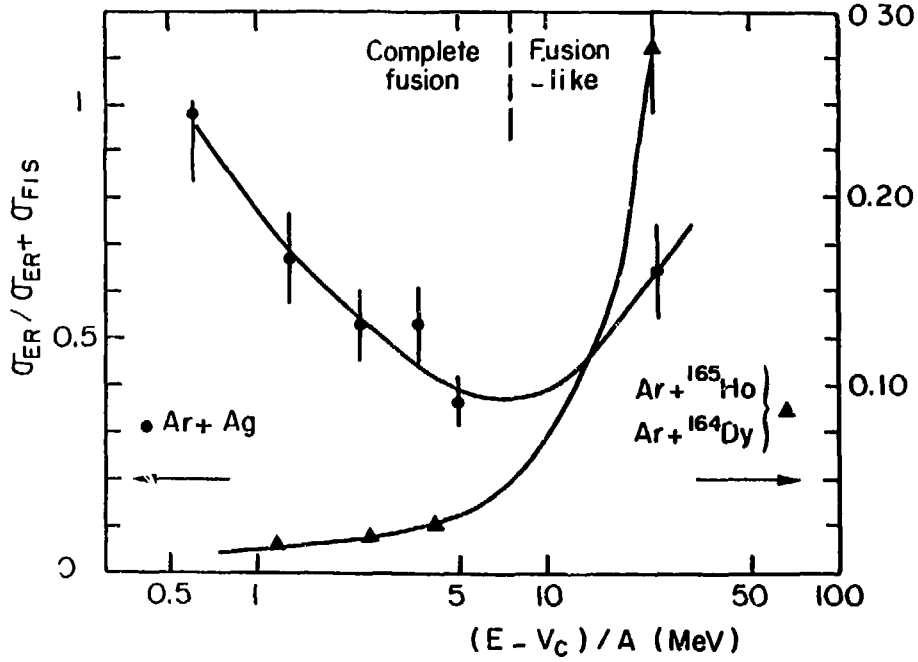
Complete fusion
Fusion - like
$\sigma_{ER} / \sigma_{ER} + \sigma_{FIS}$
1
0.5
0
0.30
0.20
0.10
• Ar+ Ag
Ar + ^{165}Ho
Ar + ^{164}Dy
0.5
1
5
10
50
100
$(E - V_C) / A$ (MeV)

Fig. 11

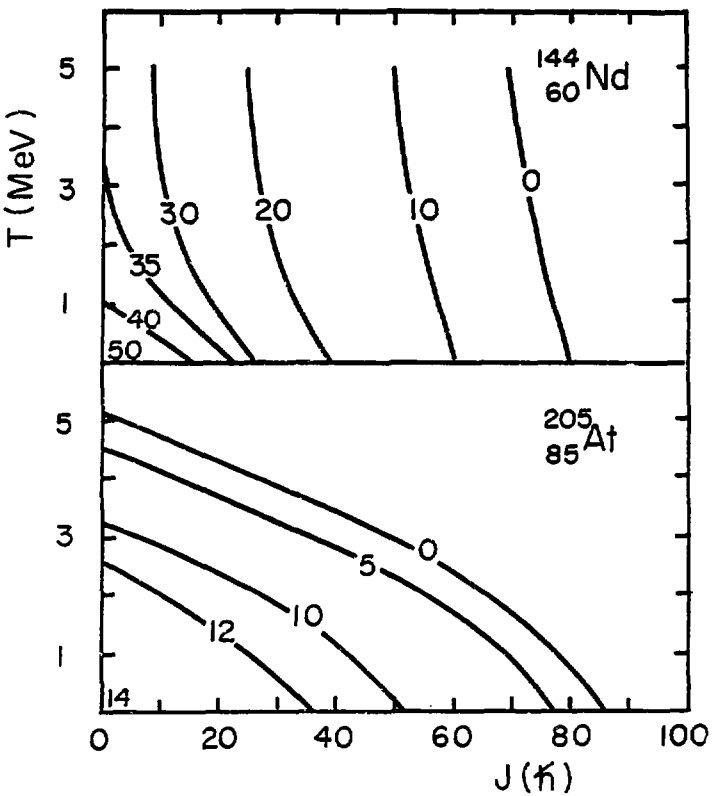
T (MeV)
5
3
1
144 60 Nd
30
20
10
0
35
40
50
205 85 At
5
0
10
12
14
0
20
40
60
80
100
J (ħ)

Fig. 12

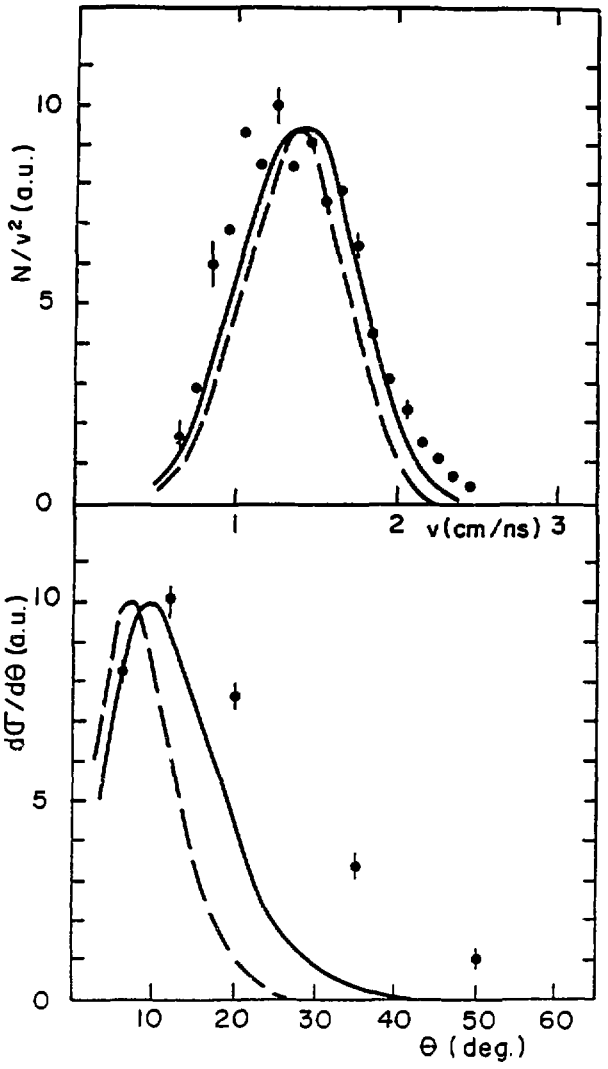

Fig. 13